

# Renormalization of the electron-spin-fluctuation interaction in the $t - t' - U$ Hubbard model

Z. B. Huang<sup>1,2</sup>, W. Hanke<sup>1</sup>, E. Arrigoni<sup>3</sup>, and A. V. Chubukov<sup>4</sup>

<sup>1</sup>*Institut für Theoretische Physik, Universität Würzburg, am Hubland, 97074 Würzburg, Germany*

<sup>2</sup>*Department of Physics, Hubei University, Wuhan 430062, PRC*

<sup>3</sup>*Institut für Theoretische Physik, Technische Universität Graz, Petersgasse 16, A-8010 Graz, Austria* and

<sup>4</sup>*Department of Physics, University of Wisconsin, Madison, Wisconsin 53706, USA*

(Dated: December 2, 2024)

We study the renormalization of the electron-spin-fluctuation (el-sp) vertex in a two-dimensional Hubbard model with nearest-neighbor ( $t$ ) and next-nearest-neighbor ( $t'$ ) hopping by a Quantum Monte Carlo calculation. Our results show that for  $t' = 0$ , the renormalized el-sp vertex decreases quite generally with decreasing temperature at all spin-fluctuation momentum transfers. The suppression of the el-sp vertex results in a substantial reduction of the effective pairing interaction mediated by antiferromagnetic spin fluctuations in both the intermediate- and strong-correlation regimes. The inclusion of a finite  $t'/t < 0$ , increases the Landau damping rate of spin fluctuations, especially in the overdoped region. The increased damping rate leads to smaller vertex corrections, in agreement with earlier diagrammatic calculations. Still, the vertex correction reduces the spin-fermion vertex, as at  $t' = 0$ .

## I. INTRODUCTION

The nature of the spin-fluctuation mediated interaction between charge carriers continues to attract high interest in the high- $T_c$  superconductivity research<sup>1,2,3,4,5,6</sup>. Theoretical calculations for the doped Hubbard and  $t - J$  models suggest that the strongest interaction between fermions is mediated by antiferromagnetic (AF) spin fluctuations. The low-energy description of this interaction has been advanced in the framework of the spin-fermion model<sup>6</sup>. A magnetically mediated interaction has been intensively studied since the early days of high  $T_c$  era because AF spin fluctuations mediate  $d$ -wave pairing between fermions<sup>1</sup>. Various numerical and analytical calculations based on Hubbard and  $t - J$  models, as well as semi-phenomenological spin-fermion models, have been performed in the normal and superconducting states of the cuprates. The results of these calculations are in quite good agreement with a large number of experimental data. In particular, these calculations show that the magnetic response in a  $d$ -wave superconducting state contains a resonance peak, in addition to a gapped continuum. The location of the peak, and its “negative” dispersion are in agreement with experimental data. It has been argued<sup>8</sup> that the scattering from the resonance is strong enough to explain the peak-dip-hump feature in the fermionic spectral function, the  $S$ -shape dispersion for antinodal fermions, and similar features in SIS tunneling, optical conductivity, and Raman response.

The strength of the feedback effects from the resonance peak on fermions, and the magnitude of spin-mediated  $T_c$  depend on the size of the spin-fermion coupling. The estimates for the coupling strength still vary substantially. Abanov *et al* argued<sup>7</sup> that the coupling  $g$  is comparable to the Hubbard  $U$  and is quite strong,  $g \sim 0.7\text{eV}$ . On the other hand, Kee *et al.*<sup>9</sup> argued that the effective spin-fermion coupling is much weaker  $g \sim 0.014\text{eV}$ . In the latter work<sup>9</sup>, the coupling was extracted from the

specific heat data. To a large extent, the difference between the two results is related to different choices for the fermionic density of states  $N_0$ : a large value of  $g$  is obtained by assuming a large, Luttinger Fermi surface, with  $N_0 \sim 1\text{eV}^{-1}$  (Ref. 7), while a smaller  $g$  results by assuming that the density of states  $N_0 \sim J^{-1} \sim 10\text{eV}^{-1}$  is the same as in weakly doped quantum AF.

This difference brings in the issue of how much the full spin-fermion vertex  $g_{\mathbf{kq}}$  (which can actually be extracted from, e.g., specific heat data) differs from the bare  $g_{\mathbf{kq}}^0$  due to vertex corrections. Here,  $\mathbf{k}$  and  $\mathbf{k} + \mathbf{q}$  are incoming and outgoing fermionic momenta, and  $\mathbf{q}$  is the bosonic momentum. The ratio  $\gamma(\mathbf{k}, \mathbf{q}) = g_{\mathbf{kq}}/g_{\mathbf{kq}}^0$  determines the vertex renormalisation originating from electronic correlations. Some of us have recently shown numerically that this quantity is substantially renormalized by strong electronic correlations both for the electron-phonon (el-ph) vertex<sup>10</sup> as well as for the el-sp vertex<sup>11</sup>.

Within the spin-fermion model, the role of vertex renormalization is well understood in the limits of very small and relatively large doping. At very small doping  $x$ , when long-range AF order is still present, nearly all carriers are localized, and doped fermions form small pockets around  $(\pi/2, \pi/2)$  and symmetry related points. In this situation, the full spin-fermion vertex  $g_{\mathbf{kq}}$  vanishes when  $\mathbf{q}$  coincides with the antiferromagnetic momentum  $\mathbf{Q} \equiv (\pi, \pi)$ . The vanishing of  $g_{\mathbf{kQ}}$  is the consequence of the Adler principle that the interaction should preserve massless Goldstone bosons in the theory and therefore should vanish at the ordering momentum of Goldstone bosons. For  $\mathbf{q} \neq \mathbf{Q}$ , the vertex is non-zero, but small in  $|\mathbf{q} - \mathbf{Q}|/|\mathbf{Q}|$ . Mathematically, the vanishing of  $g_{\mathbf{kQ}}$  is the result of dressing up of the bare interaction  $g_{\mathbf{kQ}}^0$  by coherence factors, associated with the antiferromagnetic order. From this perspective, the strong reduction of  $g_{\mathbf{kq}}$  when  $\mathbf{q}$  is close to  $\mathbf{Q}$  is the result of strong vertex renormalization. Schrieffer argued<sup>12</sup> that if the pocket-like Fermi surface survives even when long-range AF order is

lost, the strong vertex renormalization extends into the paramagnetic phase. According to Ref. 12

$$\gamma^2(\mathbf{k}, \mathbf{q}) \propto [(\mathbf{q} - \mathbf{Q})^2 + \frac{1}{\xi^2}] \sim \frac{1}{[\chi(\mathbf{q}, \omega = 0)]}, \quad (1)$$

where  $\xi$  is the AF correlation length. Once Eq. (1) is valid, the effective spin-mediated interaction

$$V(\mathbf{k}, \mathbf{q}) \propto |\gamma(\mathbf{k}, \mathbf{q})|^2 \chi(\mathbf{q}), \quad (2)$$

is considerably weaker than without vertex renormalization, and, most importantly, it is no longer peaked at  $\mathbf{q} \sim \mathbf{Q}$ . This is an important fact, since the peak structure at  $\mathbf{q} \sim \mathbf{Q}$  was responsible for a strong attractive  $d$ -wave component in the pairing potential. The magnetically-mediated  $d$ -wave pairing is still possible even in this situation, due to subleading terms in the expansion in  $\mathbf{q} - \mathbf{Q}$ , but the corresponding  $T_c$  is much smaller than one would get without vertex corrections<sup>13</sup>.

In the opposite limit of large doping, fermions are itinerant, and have a large Fermi surface which crosses the magnetic Brillouin zone boundary at hot spots (this requires a sufficiently strong next-nearest-neighbor hopping). A spin-fluctuation with momentum near  $\mathbf{Q}$  then can decay into a particle and a hole. Analytical calculations within spin-fermion model show that in this situation, the vertex is only weakly renormalized, and actually increase with respect to its bare value, i. e.  $g_{\mathbf{k}\mathbf{Q}} > g_{\mathbf{k}\mathbf{Q}}^0$ <sup>6,14</sup>. More precisely, the relation between  $g_{\mathbf{k}\mathbf{Q}}$  and  $g_{\mathbf{k}\mathbf{Q}}^0$  depends on the angle  $\phi \leq \pi$  between Fermi velocities at hot spots separated by  $\mathbf{Q}$ :

$$g_{\mathbf{k}\mathbf{Q}} = g_{\mathbf{k}\mathbf{Q}}^0 \left( 1 + \frac{\phi}{4\pi} \log \xi/\xi_0 \right), \quad (3)$$

where  $\xi_0$  is of order 1. Equation (3) shows that the renormalization is largest when  $\phi \rightarrow \pi$ . This limit corresponds to an almost nested Fermi surface at hot spots. In optimally doped cuprates, the velocities at the hot spots separated by  $\mathbf{Q}$  are almost perpendicular to each other, i.e.,  $\phi \approx \pi/2$ . For  $\xi \sim 2$ , vertex correction is then about 10% (even smaller,  $\sim 4\%$ , when one adds regular terms<sup>15,16</sup>).

The difference between the itinerant and localized limits raises the question how vertex corrections evolve as the system approaches half-filling. One attempt to address this issue was undertaken in Ref. 16. The authors of<sup>16</sup> considered a toy spin-fermion model in which one can study the evolution from the Luttinger Fermi surface towards hole pockets. This evolution involves a topological transition below which a pocket is splitted from a large Fermi surface, and Luttinger theorem breaks down. Within this model, vertex corrections evolve together with the Fermi surface: they are small and positive (i. e.  $g_{\mathbf{k}\mathbf{Q}} > g_{\mathbf{k}\mathbf{Q}}^0$ ) in the limit when the Fermi surface is large, but change their sign near the topological transition, become negative and rapidly increase in magnitude as the Fermi surface evolves towards hole pockets. For a pocket-like Fermi surface, vertex corrections almost cancel the

bare vertex, and the full  $g_{\mathbf{k}\mathbf{q}}$  coincides with Schrieffer's result, Eq. (1).

In this paper, we address the issue of the strength of vertex corrections in the two-dimensional  $t - t' - U$  Hubbard model, by means of a quite accurate numerical method – the determinantal Monte Carlo<sup>17</sup> algorithm. The purpose of our calculation is to explore the extent of validity in doping and temperature of Schrieffer's argument as well as of the spin-fermion model calculation<sup>6</sup>.

Note that the analytical results are only valid when the correlation length  $\xi$  is large, Monte-Carlo calculations are not restricted by this condition. We also want to get an insight as up to what extent a description in terms of low-energy spin degrees of freedom, i. e. in terms of a spin-fermion model is appropriate for the Hubbard model.

Our numerical Monte Carlo simulations are performed on a  $8 \times 8$  lattice at different doping densities and different temperatures. In our finite lattice, the  $(\pi, 0)$  point is the one closest to the hot spots, so that charge carriers near the  $(\pi, 0)$  region are strongly affected by antiferromagnetic spin fluctuations. Therefore, we will mainly concentrate on the particular scattering process in which the incoming electron and spin fluctuation carry momenta  $\mathbf{p} = (-\pi, 0)$  and  $\mathbf{q} = (\pi, \pi)$ , respectively. Within our  $\mathbf{p}$ -points mesh, the points  $\mathbf{p}$  and  $\mathbf{p} + \mathbf{q}$  lie sufficiently close to the Fermi surface.

Our paper is organized as follows: In Section II, we define the Hamiltonian and describe the numerical approach, which is based on the Quantum Monte Carlo evaluation of the linear response to an external spin perturbation. In Section III, we present our numerical results and discuss their qualitative relation with the spin-fermion-model calculation and Eq. 1. Finally, in Section IV, we discuss in detail our main conclusions.

## II. MODEL AND NUMERICAL APPROACH

Our starting point is the one-band Hubbard model,

$$H = -t \sum_{\langle ij \rangle, \sigma} (c_{i\sigma}^\dagger c_{j\sigma} + c_{j\sigma}^\dagger c_{i\sigma}) - t' \sum_{\langle\langle ij \rangle\rangle, \sigma} (c_{i\sigma}^\dagger c_{j\sigma} + c_{j\sigma}^\dagger c_{i\sigma}) + U \sum_i n_{i\uparrow} n_{i\downarrow}, \quad (4)$$

Here, the operators  $c_{i\sigma}^\dagger$  and  $c_{i\sigma}$  as usual create and destroy an electron with spin  $\sigma$  at site  $i$ , respectively, and  $\langle ij \rangle$  and  $\langle\langle ij \rangle\rangle$  denote a sum over nearest and next-nearest neighbor lattice sites  $i$  and  $j$ , respectively.  $n_{i\sigma} = c_{i\sigma}^\dagger c_{i\sigma}$  is the number operator. Finally,  $U$  is the onsite Coulomb interaction and we choose the nearest-neighbor hopping  $t$  as the unit of energy.

In our simulation, we use a linear-response approach (see also Ref. 10) in order to extract the el-sp vertex. In this method, one formally adds to Eq. (4) the interaction with a momentum- and (imaginary) time-dependent

spin-fluctuation field in the  $z$ -direction  $S_{\mathbf{q}}e^{-iq_0\tau^{18}}$  in the form<sup>19</sup>

$$H_{\text{el-sp}} = \sum_{\mathbf{k}\mathbf{q}\sigma} g_{\mathbf{k}\mathbf{q}}^0 \sigma c_{\mathbf{k}+\mathbf{q}\sigma}^\dagger c_{\mathbf{k}\sigma} S_{\mathbf{q}} e^{-iq_0\tau}, \quad (5)$$

where  $g_{\mathbf{k}\mathbf{q}}^0$  is the bare el-sp coupling (equal to the Hubbard  $U$  in the one-band Hubbard model). One then considers the “anomalous” single-particle propagator in the presence of this perturbation defined as<sup>18</sup>

$$G_A(p, q) \equiv - \int_0^\beta d\tau e^{i(p_0+q_0)\tau} \langle T_\tau c_{\mathbf{p}+\mathbf{q}\sigma}(\tau) c_{\mathbf{p}\sigma}^\dagger(0) \rangle_{H+H_{\text{el-sp}}}, \quad (6)$$

Here  $\langle \rangle_{H+H_{\text{el-sp}}}$  is the Green’s function evaluated with the Hamiltonian  $H+H_{\text{el-sp}}$ . Diagrammatically,  $G_A(p, q)$  has the structure shown in Fig. 1 so that the el-sp vertex  $\Gamma(p, q)$  can be expressed quite generally in terms of  $G_A$  and of the single-particle Green’s function  $G(p)$  in the form

$$\Gamma(p, q) = \lim_{S_{\mathbf{q}} \rightarrow 0} \frac{1}{g_{\mathbf{k}\mathbf{q}}^0} \frac{1}{S_{\mathbf{q}}} \frac{1}{1 + U \chi_{zz}(q)} \frac{G_A(p, q)}{G(p+q) G(p)}, \quad (7)$$

with  $\chi_{zz}(q)$  the longitudinal spin susceptibility. Due to the limit procedure in Eq. 7, it is sufficient to calculate the leading linear response of  $G_A$  to  $H_{\text{el-sp}}$ , which is given by

$$G_A(p, q) = S_{\mathbf{q}} \int_0^\beta d\tau e^{i(p_0+q_0)\tau} \int_0^\beta d\tau' e^{-iq_0\tau'} \sum_{\mathbf{k}\sigma'} g_{\mathbf{k}\mathbf{q}}^0 \times \langle T_\tau \sigma' c_{\mathbf{k}+\mathbf{q}\sigma'}^\dagger(\tau' + 0^+) c_{\mathbf{k}\sigma'}(\tau') c_{\mathbf{p}+\mathbf{q}\sigma}(\tau) c_{\mathbf{p}\sigma}^\dagger(0) \rangle_H, \quad (8)$$

where  $0^+$  is a positive infinitesimal. Notice that  $S_{\mathbf{q}}$  cancels in Eq. 7. The two-particle Green’s function in Eq. (8) is evaluated with respect to the pure Hubbard Hamiltonian (Eq. (4)).

Within a quasiparticle approach, one can shift the wave-function renormalisation factor  $Z(p) > 1$  from the Green’s function into the definition of the effective el-sp vertex

$$\gamma(p, q) = \frac{\Gamma(p, q)}{\sqrt{Z(p) Z(p+q)}}. \quad (9)$$

Numerically,  $Z(p)$  is evaluated as  $Z(p) = \text{Im}[1/G(p)]/p_0^{10,18}$ . Therefore,  $\gamma$  is the vertex between *free quasiparticles* and spin fluctuations.

The total pairing interaction  $V_p$  under the exchange of a single spin wave can be expressed in terms of the vertex  $\Gamma$  as

$$V_p(p, q) = |\Gamma(p, q)|^2 \cdot U^2 \cdot \chi_{zz}(q), \quad (10)$$

where  $\chi_{zz}(q)$  is the spin susceptibility

$$\chi_{zz}(q) = \frac{1}{2} \int_0^\beta d\tau e^{-i q_0 \tau} \langle T_\tau m_{\mathbf{q}}^z(\tau) m_{-\mathbf{q}}^z(0) \rangle,$$

and

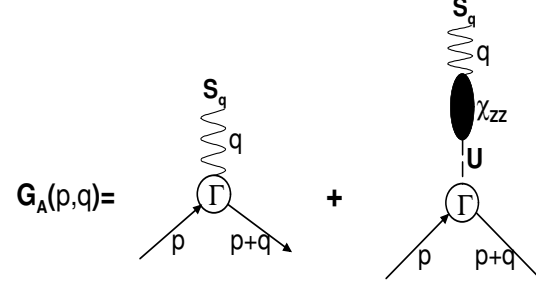


FIG. 1: Diagrammatic representation of  $G_A(p, q)$  within linear response to  $S_{\mathbf{q}}$ . The thick solid lines represent dressed single-particle Green’s functions of the Hubbard model. The wavy line denotes the external perturbation in Eq. (5). The dashed line represent the Hubbard interaction  $U$  and the black ellipse stands for the longitudinal spin susceptibility  $\chi_{zz}(q)$ .

$$m_{\mathbf{q}}^z = \frac{1}{\sqrt{N}} \sum_{\mathbf{k}\sigma} \sigma c_{\mathbf{k}+\mathbf{q}\sigma}^\dagger c_{\mathbf{k}\sigma}. \quad (11)$$

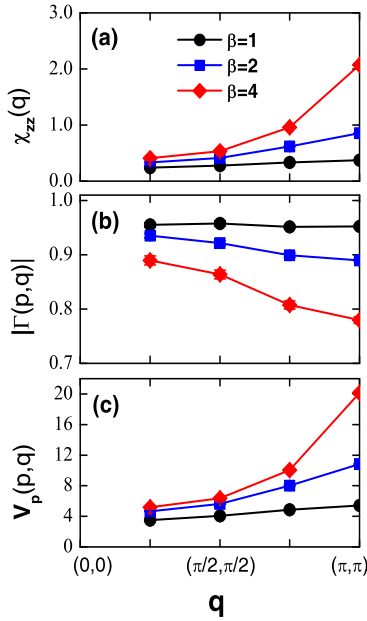
Eq. 10 describes the effective pairing interaction between *dressed fermions*. Including the wave-function renormalisation as in Eq. 9, we can define the effective pairing interaction *between free quasiparticles* as

$$V(p, q) = \frac{V_p(p, q)}{Z(p) Z(p+q)}. \quad (12)$$

Clearly, both  $V_p(p, q)$  and  $V(p, q)$  contain the contributions from both the real and imaginary parts of the vertex.

### III. RESULTS AND DISCUSSIONS

In order to explore the momentum structure of the el-sp interaction, we first plot  $\chi_{zz}(q)$ ,  $|\Gamma(p, q)|$ , and  $V_p(p, q)$  versus  $\mathbf{q}$  at different temperatures in Fig. 2. Here, the spin-fluctuation momentum transfer  $\mathbf{q}$  is along the  $(1, 1)$  direction. One can readily see that both  $\chi_{zz}(q)$  and  $V_p(p, q)$  are peaked at momentum transfers around the antiferromagnetic vector  $\mathbf{Q} = (\pi, \pi)$ , and the strength of the peaks increases when the temperature is lowered. This demonstrates that the  $\mathbf{q}$ - and  $T$ -dependences of the spin susceptibility  $\chi$  dominate the temperature behavior of the pairing interaction, despite the reduction of the vertex  $\Gamma$  as the temperature is decreased. From Fig. 2, we observe that the decrease with temperature of  $\Gamma$  at large momentum transfers is stronger than at small momentum transfers, indicating that the vertex correction at  $\mathbf{q} \sim \mathbf{Q}$  is larger than at small  $\mathbf{q}$ . This  $\mathbf{q}$ -dependence of the el-sp vertex is qualitatively in agreement with the prediction of Eq.(1). Our finding is also in good agreement with the work of Bulut *et al.*<sup>20</sup>, which shows a value of  $g = 0.8$  (corresponding  $|\Gamma| = 0.8$  in our notation) can produce an effective coupling  $gU$  which is consistent with the results of Monte Carlo calculation of the irreducible particle-hole vertex, and that the effective particle-particle interaction



originating from the Hubbard  $U$  increases with lowering temperature and can reach large values.

Monte Carlo results for  $\Gamma(p, q)$ ,  $\gamma(p, q)$ ,  $Z(p)$ ,  $V_p(p, q)$  and  $V(p, q)$  are displayed in Figs. 3 and 4. We notice that in the underdoped regime ( $\delta = 0.12$ ) for both intermediate ( $U = 4$ ) and strong correlation ( $U = 8$ ), both  $\Gamma$  and  $\gamma$  are strongly renormalized below a characteristic temperature ( $T \lesssim J = 0.5$  for  $U = 8$ ). Although our simulation cannot reach low temperatures, a clear trend is observable in both  $\text{Re}\Gamma$  and  $\text{Re}\gamma$ , which tend to go to a very small value at low temperatures, at least for  $U = 8$ . At our lowest accessible  $T$ 's,  $\text{Im}\Gamma(p, q)$  and  $\text{Im}\gamma$  are small at weak and intermediate correlations, but for  $U = 8$  they can become comparable to the real part. Our numerical results presented in Fig. 4 clearly show that, in both intermediate- and strong-correlation regimes, the total pairing interaction  $V_p$  is smaller than the RPA result obtained with the full susceptibility  $\chi_{zz}$ . The difference becomes strongest at the lowest accessible temperatures. The qualitative temperature behavior of the effective pairing interaction between quasiparticles  $V$ , is quite similar to  $V_p$  in the intermediate-correlation ( $U = 4$ ) regime. However, it is quite different in the strong-correlation ( $U = 8$ ) regime, where it displays a mild increase or a saturation at low  $T$ 's. Based on the results shown in Fig. 4, we can conclude that vertex corrections are crucial for the spin-mediated pairing inter-

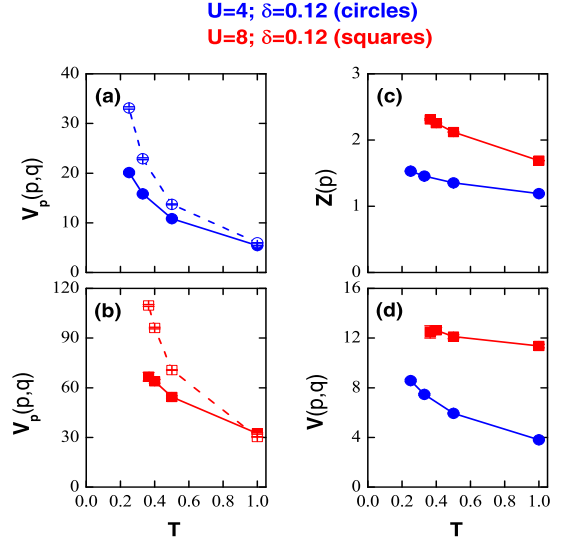
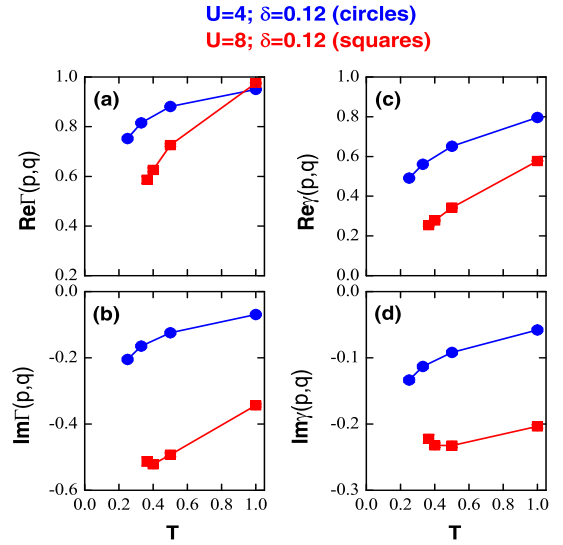


FIG. 4: (color online) Total pairing interaction  $V_p(p, q)$  vs  $T$  for (a)  $U = 4$  and (b)  $U = 8$  at the doping density  $\delta = 0.12$  (full symbols, the solid line is a guide to the eye). The open symbols (dashed line) show the RPA results. In panel (c), we show the  $T$ -dependence of the wave-function renormalization  $Z(p)$  and in panel (d) the effective pairing interactions  $V(p, q)$  between quasiparticles. In all panels,  $\mathbf{p} = (-\pi, 0)$ ,  $\mathbf{q} = (\pi, \pi)$ , and  $t' = 0$ .

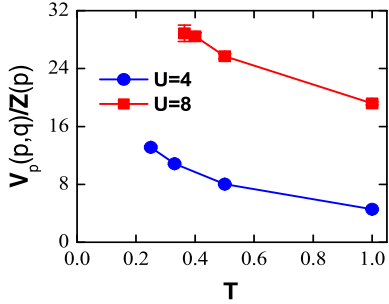


FIG. 5: (color online)  $V_p(p, q)/Z(p)$  vs  $T$  for  $U = 4$  and  $U = 8$  at the doping density  $\delta = 0.12$  (full symbols, the solid line is a guide to the eye).  $\mathbf{p}$  and  $\mathbf{q}$  are the same as in Fig. 4.

action, as they produce a strong suppression of  $V_p$  and an order of magnitude reduction [ $\sim O(10)$ ] in  $V$ .

The pairing strength is proportional to the effective quasiparticle interaction  $V$  times the density of states at the Fermi level  $N(E_F)$ . In a Fermi-liquid picture, the latter is increased by a factor  $Z$  with respect to the non-interacting density of states  $N_0(E_F)$ . A measure of this strength is thus given by  $N(E_F) V \propto N_0(E_F) Z V = N_0(E_F) V_p/Z$ . As one can see, the latter term contains a correction due to electronic correlation, which is similar to the correction occurring in the McMillan formula for the case of the electron-phonon mediated pairing in the strong-coupling case. In order to have a measure of the pairing strength including the renormalisation of the density of states, we thus plot the quantity  $V_p(p, q)/Z(p)$  in Fig. 5 as a function of temperature for  $\delta = 0.12$ . We observe that  $V_p(p, q)/Z(p)$  increases with decreasing temperature in both intermediate- and strong-correlation regimes. On the other hand, the strong suppression of  $V_p$  due to vertex corrections and the increase of  $Z$  with decreasing temperature reduce considerably the pairing strength in comparison to the RPA case (i. e., without vertex corrections), in particular in the low-temperature regime.

Our results plotted in Fig. 4, show that vertex corrections are still rather dramatic even in the case in which the AF correlation length  $\xi$  is quite small<sup>21</sup>. i. e. of order of the Cu-Cu distance. This is in contrast to the situation discussed by Schrieffer in which holes move in an AF background, which is unaffected by the charge carriers, i. e.  $\xi$  is large. How can we understand this result? In the AF precursor (large- $\xi$ ) case<sup>12,16</sup>, the vanishing of the el-sp interaction in the long-range ordered AF state is the result of dressing up of the bare interaction by the AF coherence factor, which is small at the top of the valence band, as pointed out by Schrieffer and Chubukov. The coherence factor is due to the interference effect of the quasiparticle, which forms a “spin-bag”, i.e. a hole dressed by a short-range AF background. Although in our calculation the AF precursor is no longer

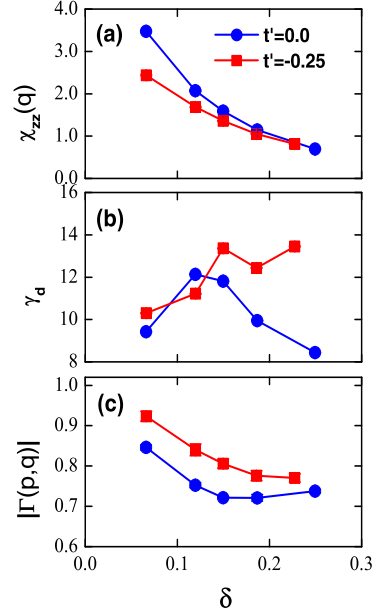


FIG. 6: (color online) (a) Spin susceptibility  $\chi_{zz}(q)$ , (b) “damping rate”  $\gamma_d$ , and (c) el-sp vertex  $|\Gamma(p, q)|$  as a function of doping density  $\delta$  for  $U = 4$ . The value of  $t'$  is indicated by the shape of the symbol. Here  $\mathbf{p} = (-\pi, 0)$ ,  $\mathbf{q} = (\pi, \pi)$ , and  $\beta = 4$ .

present, it is well established from our earlier QMC work on the evolution of the single-particle spectral function  $A(\mathbf{k}, \omega)$ <sup>21</sup> from an insulator to a metal that below  $T \sim J$ , the electronic excitations display an essentially doping-independent feature. More precisely, a “band” of width  $J$  forms, in which “spin-bag”-like quasiparticles propagate coherently. The continuous evolution can be traced back to one and the same many-body origin: the doping-dependent AF spin-spin correlation. Therefore, we argue that the interference effect of the spin-bag quasiparticle plays a similar role in reducing the el-sp vertex in the strongly-correlated underdoped regime.

As discussed in the introduction, previous work on the spin-fermion model<sup>6</sup> suggests that the vertex correction  $|\Gamma - 1|$  (not including  $Z$ ) gets considerably reduced whenever spin fluctuations get damped. To explore this fact, we have compared numerical results for different values of the next-nearest-neighbor hopping ( $t' = 0$  and  $t' = -0.25$ ), since one expects the damping to increase for larger negative  $t'$ . The spin susceptibility  $\chi_{zz}$ , a quantity proportional to the damping rate  $\gamma_d$ , and the el-sp vertex  $\Gamma$  are plotted in Figs. 6(a)-6(c) as a function of doping density. When  $t' = 0$ , the Fermi surface is particlelike and encloses the zone center  $\Gamma = (0, 0)$ . On the other hand, when  $t' = -0.25$ , the Fermi surface is holelike and encloses the zone corner  $Q = (\pi, \pi)$ , and, in particular, it crosses the magnetic Brillouin Zone boundary at so-called hot spots. In this second case, spin fluctu-

ations get strongly damped due to the decay into particle and holes near the Fermi surface. Due to the finite temperature and short correlation length, a damping of spin fluctuations is also present for  $t' = 0$ . The quantity  $\gamma_d = b/c$  shown in Fig. 6, is obtained by fitting the spin susceptibility  $\chi(q, i\omega_m)^{-1}$  to the form  $a + b\omega_m + c\omega_m^2$ , and is, thus, proportional to the spin damping rate. In the underdoped region, the spin susceptibility is strongly suppressed by a negative  $t'$  due to its frustration effect on the AF alignment, whereas the difference of  $\gamma_d$  is small, as seen in Fig. 6(a) and Fig. 6(b). On the other hand, in the overdoped region, where the holelike Fermi surface passes close to  $(\pi, 0)$  and symmetry points, whereas the particlelike Fermi surface moves away from the magnetic Brillouin zone boundary,  $t'$  has little effect on the spin susceptibility, while the spin damping rate is dramatically increased by a negative  $t'$ . Fig. 6(c) clearly shows that the el-sp vertex  $|\Gamma|$  is larger for  $t' = -0.25$  than for  $t' = 0$ , demonstrating that the vertex correction is reduced either by suppressing the spin susceptibility or by increasing the spin damping rate. However, the largest difference in  $|\Gamma|$  is not observed at the smallest doping density  $\delta = 0.066$ , where the suppression of the spin susceptibility is strongest, or near the doping density  $\delta = 0.20$ , where the difference of the damping rates is largest. This result suggests that, although both the spin susceptibility and the damping of spin fluctuations are related to the magnitude of vertex corrections, they are probably not the only relevant factors.

Finally, we would like to remark the overall sign of the vertex correction. In our studied cases, as shown in Fig. 2 and Fig. 6,  $|\Gamma|$  is always less than 1, indicating that the el-sp interaction is suppressed by vertex corrections. This is in contrast to the finding in the spin-fermion model, which shows that the total vertex correction at moderate doping has a positive sign, i.e., vertex correction actually increases the el-sp interaction. This effect, however, is rather small and for moderate  $\xi$  may be overshadowed by the contributions from high-energies ( $O(E_F)$ ), not included in the low-energy spin-fermion models. The comparison between our calculations and the results in the spin-fermion model shows that while the effect of damping of spin fluctuations on vertex corrections is quite robust and agrees with low-energy considerations, the sign

and the magnitude of the vertex correction near optimal doping may be model dependent.

#### IV. CONCLUSIONS

In summary, based on quantum Monte Carlo simulations, we have studied the renormalization of the el-sp vertex in the two-dimensional  $t - t' - U$  Hubbard model. We found that the renormalized el-sp vertex decreases quite generally with decreasing temperature at all spin-fluctuation momentum transfers. The suppression of the el-sp vertex results in a substantial reduction of the pairing mediated by antiferromagnetic spin fluctuations in both the intermediate- and strong-correlation regimes. This result extends Schrieffer's argument Eq. 1 about the suppression of the el-sp vertex to the case in which the AF precursor is no longer present. Notice, however, that the result that  $\gamma$  and  $\chi$  behave in the opposite way, as expressed by Eq. 1, only holds when considering their *temperature* behavior. In contrast, when decreasing *doping* at fixed temperatures, while  $\chi$  increases,  $\gamma$  remains quite flat, as can be seen in Fig. 4 of our previous work, Ref.<sup>11</sup>. Thus, in the present case in which the system is away from the AF precursor, there is no general proportionality relation as implied in Eq. 1. This is consistent with the spin-bag picture discussed above, which is expected to be rather doping independent as well.

By adding a negative next-nearest-neighbor hopping term  $t'/t$ , we observe that the damping of spin fluctuations reduces vertex corrections, in agreement with previous results on the spin-fermion model. However, in contrast to Ref.<sup>6</sup>, we do not observe a positive vertex correction, i. e.  $|\Gamma|$  is always less than 1.

We thank D.J. Scalapino for useful discussions. The Würzburg group acknowledges support by the DFG under Grant No. DFG-Forschergruppe 538, by the Bavaria California Technology Center (BaCaTeC), and the KONWHIR project CUHE. The work of Z.B.H was supported in part by the National Science Foundation Grant No. 10574040. The calculations were carried out at the high-performance computing centers LRZ (München) and HLRS (Stuttgart).

<sup>1</sup> D.J. Scalapino, Physics Reports **250**, 329-365 (1995).

<sup>2</sup> M. Imada, A. Fujimori, and Y. Tokura, Rev. Mod. Phys. **70**, 1039 (1998).

<sup>3</sup> F. Assaad, W. Hanke, and D. J. Scalapino, Phys. Rev. Lett. **71**, 1915 (1993), and Phys. Rev. B **50**, 12835 (1994).

<sup>4</sup> M. Eschrig and M.R. Norman, Phys. Rev. Lett. **85**, 3261 (2000).

<sup>5</sup> J. Carbotte, E. Schachinger, and D.N. Basov, Nature (London) **401**, 354 (1999).

<sup>6</sup> Ar. Abanov, A.V. Chubukov, and J. Schmalian, Adv. in Phys. **52**, 119 (2003).

<sup>7</sup> Ar. Abanov *et al.*, Phys. Rev. Lett. **89**, 177002 (2002).

<sup>8</sup> Ar. Abanov, A.V. Chubukov, and J. Schmalian, Journal of electron spectroscopy and related phenomena, v117, p129 (2001); A. Chubukov and M.R. Norman, Phys. Rev. B, **70**, 174505 (2004).

<sup>9</sup> H.Y. Kee, S.A. Kivelson, and G. Aeppli, Phys. Rev. Lett. **88**, 257002 (2002).

<sup>10</sup> Z.B. Huang, W. Hanke, E. Arrigoni, and D.J. Scalapino, Phys. Rev. B **68**, 220507(R) (2003).

<sup>11</sup> Z.B. Huang, W. Hanke, and E. Arrigoni, Europhys. Lett. **71** (6), pp.959 (2005).

<sup>12</sup> J.R. Schrieffer, J. Low Temp. Phys. **99**, 397 (1995).

<sup>13</sup> O.P. Sushkov and V. Kotov, Phys. Rev. B **70**, 024503 (2004) and references therein.

<sup>14</sup> B.L. Altshuler, L.B. Ioffe, and A.J. Millis, Phys. Rev. B **52**, 5563 (1995).

<sup>15</sup> A.V. Chubukov, P. Monthoux, and D.K. Morr, Phys. Rev. B **56**, 7789 (1997).

<sup>16</sup> A.V. Chubukov and D.K. Morr, Physics Reports **288**, 355 (1997).

<sup>17</sup> R. Blankenbecker, D.J. Scalapino, and R.L. Sugar, Phys. Rev. D **24**, 2278 (1981).

<sup>18</sup> In our convention, unbolted variables denote both Mat- subara frequency and momentum, i.e.,  $p = (p_0, \mathbf{p})$  and  $q = (q_0, \mathbf{q})$ . We have set the frequencies to their minimum values, i.e.,  $p_0 = \pi T$  for fermions and  $q_0 = 0$  for bosons.

<sup>19</sup> The imaginary-time-dependent perturbation (5) has a well-defined meaning within a functional-integral formulation, where it leads to the linear-response result (8).

<sup>20</sup> N. Bulut, D.J. Scalapino, and S.R. White, Phys. Rev. B **47**, 2742 (1993).

<sup>21</sup> C. Gröber, R. Eder, and W. Hanke, Phys. Rev. B **62**, 4336 (2000); R. Preuss, W. Hanke, C. Gröber, and H.G. Evertz, Phys. Rev. Lett. **79**, 1122 (1997).